Journal of the Korean Ceramic Society
Vol. 48, No. 4, pp. 282~287, 2011.

DOI:10.4191/KCERS.2011.48.4.282

Effect of ACF and WO_3 from ACF/WO_3/TiO_2 Composite Catalysts on the Photocatalytic Degradation of MO Under Visible Light

Ze-Da Meng, Da-Ye Song, Lei Zhu, Chong-Yeon Park, Jong-Geun Choi, and Won-Chun Oh†

Department of Advanced Materials Science & Engineering, Hanseo University, Seosan 356-706, Korea

(Received June 27, 2011; Resived July 21, 2011; Accepted July 21, 2011)

ABSTRACT

ACF and WO_3 modified TiO_2 composites (ACF/WO_3/TiO_2) were prepared using a sol-gel method. The composites were characterized by Brunauer–Emmett–Teller (BET) surface area measurements, X-ray diffraction (XRD), energy dispersive X-ray (EDX) analysis and scanning electron microscope (SEM) analysis. A methyl orange (MO) solution under visible light irradiation was used to determine the photocatalytic activity. The degradation of the MO was determined using UV/Vis spectrophotometry. An increase in photocatalytic activity was observed and attributed to an increase of the photo-absorption effect by the WO_3 and the cooperative effect of the ACF.

Key words : WO_3, ACF, MO, Visible light, Photocatalytic

1. Introduction

Semiconductor oxides have been widely used in optical coating and microelectronic devices, and using them for purifying contaminants in air and water has been recognized recently.[1-4] Photocatalytic reactions of semiconductors, such as splitting water and decomposing waste materials have received special attention because of the possible application to the conversion of solar energy into chemical energy and pollution control using solar energy.[5,6] In these investigations, various semiconductor materials, such as TiO_2, CdS, ZnS, ZnO and WO_3, have been used to study photocatalytic reduction of pollution in water,[7-11] among which TiO_2 was proved to be the most efficient photocatalyst due to its exceptional optical and electronic properties, chemical stability, non-toxicity, and low cost.[12-14] TiO_2 shows the highest quantum yield among the popular semiconductors. However, in many cases, the photocatalytic activity of TiO_2 is not enough to be useful for industrial purposes.[15-17]

The general photocatalytic process of a semiconductor involves forming photoinduced electrons at the conduction band and holes at the valence band, and the subsequent chemical reactions with the surrounding media after photo-stimulated charges move to the powder surface. In this way, water can be split into hydrogen and oxygen, and organic pollutants in water or gas can be effectively decomposed or purified. Thus, an efficient photocatalytic process over a semiconductor demands the high mobility for photoinduced electron-hole separation and for their transportation in a crystal lattice, which would lower the probability for electron-hole recombination.[18-20]

WO_3 has attracted much attention because it shows an appropriate band gap energy level (2.8 eV) and also has a lower conduction band (E_{CB} = + 0.4 V_{VS}) than that of TiO_2. Many studies on the combined semiconductors for an efficient electron-hole separation have been reported using WO_3 with coupled materials, such as WO_3/$SrNb_2O_6$ and WO_3/TiO_2.[21-24]

Moreover, activated carbon fiber (ACF) is highly microporous and has a high surface area, a larger pore volume and a uniform microspore size distribution.[25] TiO_2 particles have been easily fixed on ACF surfaces and thus have improved defects at low interface areas.[26] Thus ACF/TiO_2 composistes are typically used to obtain the combined effects of photo activity.

In the present work, the ACF/WO_3/TiO_2 photocatalyst was prepared with the sol-gel method and the photocatalytic activity for the MO solution was investigated under visible light irradiation. The effect of the composition was tested to clarify the mechanism of the charge separation process. X-ray diffraction (XRD), scanning electron microscopy (SEM) and energy dispersive X-ray (EDX) spectroscopy were used to characterize the new complexes.

2. Experimental Procedure

2.1. Materials

ACFs were obtained from the EAST ASIS Carbon Fibers Co., (Ltd, An Shan, China), and used as the carbon matrix. Titanium (IV) oxysulfate hydrate ($TiOSO_4 \cdot _X H_2O$ (TOS), Sigma-Aldrich, Germany) was used as the titanium source. The ammonium metatungstate hydrate ($H_{26}N_6O_{40}W_{12} \cdot xH_2O$) purchased from Sigma-Aldrich™ Chemie GmbH (Germany) was used as a raw material to generate WO_3 at high temperatures. The methyl orange (MO, $C_{14}H_{14}N_3NaO_3S$, 99.9%, Duksan Pure Chemical Co., Ltd) was of analytical grade.

†Corresponding author : Won-Chun Oh
E-mail : wc_oh@hanseo.ac.kr
Tel : +82-41-660-1337 Fax : +82-41-688-3352

2.2. Preparation of ACF/WO_3 composites

These ACFs were washed with deionized water and dried for 24 h at ambient temperature. The ACFs were pulverized by a pulverizer. 20 g of carbon fiber materials were ball milled for 48 h at room temperature in a laboratory tumbling ball mill, and then the mechano-chemically carbon materials were obtained using a laboratory Pulverisette 6 mono-planetary high energy mill (Idar-Oberstein, Frisch, Germany) for 1 h with ZrO_2 ball (1 mm × 300 g). 20 g of carbon fiber materials were ball-milled for 48 h at room temperature in a laboratory tumbling ball mill, and then the mechano-chemically carbon materials were obtained using a laboratory Pulverisette 6 mono-planetary high energy mill (Idar-Oberstein, Frisch, Germany) for 1 h with ZrO_2 ball (1 mm × 300 g). H_2SO_4 and H_3PO_4 mixed solution (volume ratio of 70 : 30, solution A) was used to oxidize the ACF particles. 10 g of pulverized ACF were mixed with 100 ml of solution A, stirred 7-8 hours and flushed with distilled water three times and dried at 323 K. Oxidized ACFs were formed.

For WO_3 coating, 3.8×10^{-3} mol $H_{26}N_6O_{40}W_{12}{\cdot}xH_2O$ was added to 50 ml of distilled water (shown in Table 1). The resulting mixture was heated under reflux in air and stirred at 343 K for 6 h using a magnetic stirrer in a vial. After heat treatment (N_2 atmosphere) at 623 K for 3 h, the ACF/WO_3 composites were formed.

2.3. Preparation of ACF/WO_3/TiO_2 composites

ACF/WO_3 was prepared using pristine concentrations for the preparation of ACF/WO_3/TiO_2 composites. ACF/WO_3 powder was mixed with 100 ml of 0.1 M TOS solution. The mixture was homogenized under reflux at 343 K for 3 h, while being stirred in a vial. After stirring, the solution transformed to ACF/WO_3/TiO_2 gels and heat treated (N_2 atmosphere) at 773 K to produce the ACF/WO_3/TiO_2 composites.

2.4. Characterization of ACF/WO_3/TiO_2 compounds

XRD (Shimata XD-D1, Japan) was used for crystal phase identification and to estimate the anatase ratio of TiO_2 and estimate the crystal phase of WO_3. The XRD patterns were obtained at room temperature using Cu Kα radiation. SEM (JSM-5200, JOEL, Japan) was used to observe the surface state and porous structure of the ACF/WO_3/TiO_2 composites. The elemental composition of the ACF/WO_3/TiO_2 composites was examined by EDX. SEM was used to observe the surface state and structure of the ACF/WO_3/TiO_2 composites using a scanning electron microscope (JSM-5200, JOEL, Japan). The Brunauer-Emmett-Teller (BET) surface area was determined by N_2 adsorption measurements at 77 K (Monosorb, USA).

Table 1. Nomenclature of the Samples Prepared with the Photocatalysts

Preparation method	Nomenclatures
10 g ACF + 3.8×10^{-3} mol $H_{26}N_6O_{40}W_{12}{\cdot}xH_2O$	ACF/WO_3
3.8×10^{-3} mol $H_{26}N_6O_{40}W_{12}xH_2O$ + 100 ml (0.1 M) TOS	WO_3/TiO_2
10 g ACF + 3.8×10^{-3} mol $H_{26}N_6O_{40}W_{12}{\cdot}xH_2O$ + 100 ml (0.1 M) TOS	ACF/WO_3/TiO_2

2.5. Photocatalytic tests

A specified quantity of the photocatalyst composite was added to 100 ml of MO solution. The reactor was placed in the dark for 2 h to allow the maximum adsorption of MO molecules to the photocatalyst composite particles. In all the experiments, the initial concentration of the MO was 1×10^{-5} mol/L, and the amount of the photocatalyst composite was 0.01 g/(100 ml solution). After adsorption, photodecomposition of the MO solution was performed under visible light in a dark-box to ensure that the reactor was irradiated by a single light source. The visible light source was an 18 W lamp with the main emission wavelength was 460 nm. Visible light irradiation of the photoreactor was performed for 10 min, 30 min, 60 min, 90 min, 120 min, and 150 min. The experiments were performed at room temperature. In the process of MO degradation, a glass reactor was used and the reactor was placed on a magnetic churn dasher. Samples were then withdrawn regularly from the reactor and the dispersed powders were removed by a centrifuge. The MO concentration in the solution was then determined as a function of the irradiation time from the change in absorbance at a wavelength of 660 nm. After treatment with the centrifuge the centrifugalizations were analyzed using a UV-vis spectrophotometer.

3. Results and Discussion

3.1. Elemental analysis of the preparation

Fig. 1 shows the EDX patterns of the ACF/WO_3, WO_3/TiO_2 and ACF/WO_3/TiO_2 (c). The elemental composition of these samples was analyzed and the characteristic elements were identified. Fig. 1 shows strong Kα and Kβ peaks from Ti at 4.51 and 4.92 keV, whereas a moderate Kα peak for O appears at 0.52 keV.[27] In addition to the above peaks, Ni was also observed. Fig. 1 presents the quantitative microanalysis of C, O, Ti and Ni as the major elements for the composites by EDX. Table 1 lists the composition ratios of the samples. There were some small impurities, which are believed to have been introduced from the unpurified ACF or $H_{26}N_6O_{40}W_{12}{\cdot}xH_2O$. In most of the samples, tungsten, carbon and titanium were present as major elements with small quantities of oxygen in the composite (shown in Table 2).

3.2. Surface characteristics of the samples

Fig. 2 shows the SEM images of the micro-surface structures and the morphology of the compounds. The TiO_2 and ACF particles were coated uniformly over the tungsten oxide surface, which led to an increase in nanoparticle size. Zhang et al. reported that a good dispersion of small particles could provide more reactive sites for the reactants than aggregated particles.[28] The surface roughness appears to be high due to some grain aggregation. We did not find ACF particles from the SEM image because the content of ACF was so small (Table 2). Figs. 2(a), (b) and (c) show the SEM images of

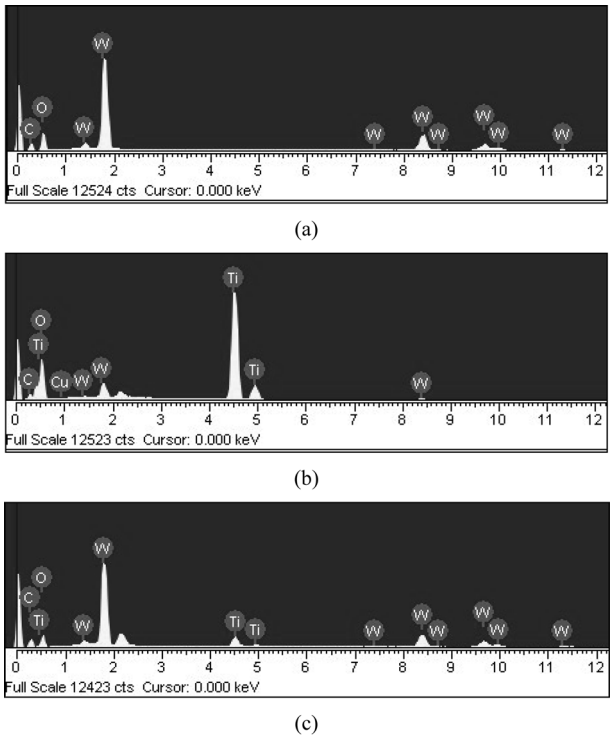

Fig. 1. EDX elemental microanalysis of the photocatalysts.

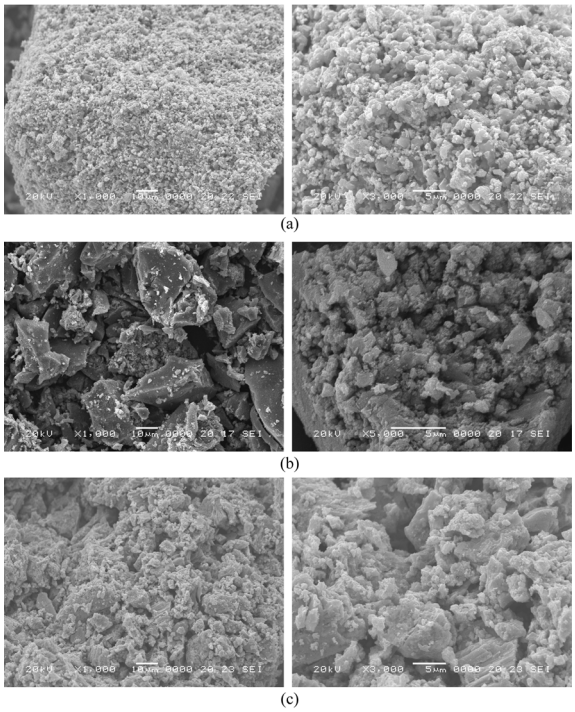

Fig. 2. SEM images of ACF/WO_3 (a) WO_3/TiO_2 (b) and ACF/WO_3/TiO_2 (c) composites.

Table 2. EDX Elemental Microanalysis and BET Surface Area

Sample name	C (%)	O (%)	W (%)	Impurity (%)	Ti (%)	BET (m^2/g)	k_{app}
TiO_2	_	_	_	0.01	99.99	18.95	2.24×10^{-4}
ACF/WO_3	54.08	17.25	22.92	5.75	_	73.25	2.86×10^{-3}
WO_3/TiO_2	27.24	36.71	_	0.02	58.82	32.20	1.52×10^{-3}
ACF/WO_3/ TiO_2	10.41	35.28	3.22	1.03	50.06	50.11	4.75×10^{-3}

ACF/WO_3, WO_3/TiO_2 and ACF/WO_3/TiO_2, respectively. The level of aggregation increased with an increasing amount of addition. Comparing Figs. 2(a), (b) and (c), we see that when TiO_2 was added, the aggregation became stronger. TiO_2 can enhance aggregation.

Table 2 lists the BET surface areas of the samples. The BET surface areas of pristine TiO_2, as well as the prepared ACF/WO_3, WO_3/TiO_2 and ACF/WO_3/TiO_2, were 18.95 m^2/g, 73.25 m^2/g, 32.20 m^2/g and 50.11 m^2/g, respectively. The TiO_2 and WO_3 particles were introduced to the pores of the ACF, which decreased the BET surface area. The ACF/WO_3 sample had the largest area, which can affect the adsorption reaction. The BET surface area of the photocatalyst ACF/WO_3/TiO_2 decreased by 31.59% when ACF/WO_3 particles were doped by TiO_2. This is because TiO_2 particles filled the pores of the ACF/WO_3 particles,[29] thereby reducing the pore size and pore volume of the ACF/WO_3 particles (Table 2).

3.3. Structural analysis

Fig. 3 shows XRD patterns of the ACF/WO_3, WO_3/TiO_2 and ACF/WO_3/TiO_2 composites. After heat treatment at 873 K, major peaks were observed at 25.3°, 37.9°, 48.0°, 53.8°, 54.9°, and 62.5°(2θ), which were assigned to the (101), (004), (200), (105), (211), and (204) planes of anatase, indicating that the prepared TiO_2 is anatase.[30-33] These results suggest that ACF/WO_3/TiO_2 also has a pure anatase phase structure with the current preparation conditions. The XRD pattern shows the

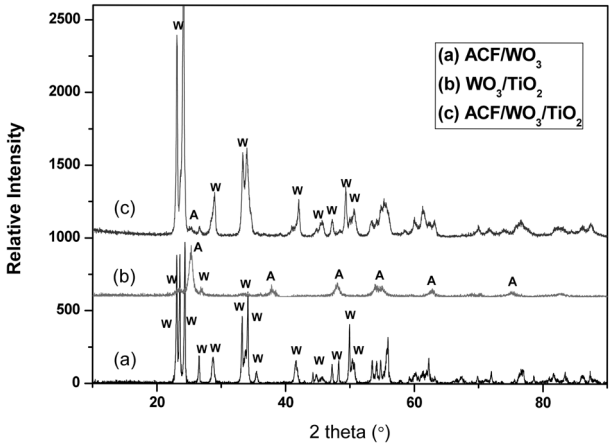

Fig. 3. XRD patterns of ACF/WO_3, WO_3/TiO_2 and ACF/WO_3/TiO_2 composites.

characteristic peaks of WO_3. Additional WO_3 diffraction peaks for the (002), (020), (200), (120), (112), (022), (–202), (202), (122), (222), (320), (123), (312), (004), (040), (140), (–114) and (114) planes were observed at 23.14°, 23.47°, 24.29°, 26.53°, 28.67°, 33.3°, 34.5°, 35.45°, 41.48°, 44.27°, 44.66°, 45.70°, 47.24°, 48.25°, 49.93°, 50.34° and 50.74° (2θ), respectively.[34-37] The peaks of TiO_2 were also observed in the XRD pattern of the ACF/WO_3/TiO_2 compound at 37.9° (2θ). In the XRD pattern of the WO_3/TiO_2 and ACF/WO_3/TiO_2 composites, the intensity of the peaks about TiO_2 was decreased. This is because the content of TiO_2 was decreased, and the peaks of WO_3 affected the TiO_2 peak. There were a few other peaks which were probably introduced from the unpurified ammonium metatungstate hydrate and $TiOSO_4$·xHO_2.[38]

3.4. Photocatalytic activity of samples

Fig. 4 shows the times of the MO degradation using pure TiO_2, ACF/WO_3, WO_3/TiO_2 and ACF/WO_3/TiO_2 under visible light irradiation. The spectra for the MO solution after visible light irradiation showed relative degradation yields at different irradiation times. The decrease in dye concentration continued with an oppositely gentle slope, which was due to visible light irradiation. The concentration of MO was 1.0×10^{-5} mol/l, the absorbance for MO decreased with an increasing visible light irradiation time. Moreover, the MO solution increasingly lost its color, and the MO concentration continued to decrease. Two steps are involved in the photocatalytic decomposition of dyes: the adsorption of dye molecules and degradation. After adsorption in the dark for 2 h, the samples reached adsorption-desorption equilibrium. In the adsorptive step, the ACF/WO_3, WO_3/TiO_2 and ACF/WO_3/TiO_2 composites showed adsorptive effects different from ACF/WO_3 and had the best adsorptive effect. The adsorptive effect of pure TiO_2 was the lowest. ACF/WO_3 has the largest BET surface area, which can enhance the adsorptive effect. In the degradation step, the ACF/WO_3, WO_3/TiO_2 and ACF/WO_3/TiO_2 composites showed a good degradation effect. A comparison of the decoloration effect of the catalysts showed that ACF/WO_3/TiO_2 composites have best degradation effect, which is due to the synergistic reaction of WO_3, ACF and TiO_2.

Fig. 5 presents the corresponding $-\ln(C/C_0)$ vs. t plots at 0-120 min irradiation times. The photodegradation followed first-order kinetics. The kinetics can be expressed as follows: $-\ln(C/C_0) = k_{app}t$ where k_{app} is the apparent reaction rate constant, C and C_0 are the initial concentration and the reaction concentration of MO, respectively. Table 2 shows the rate constant values (k_{app}) of pure TiO_2, ACF/WO_3, WO_3/TiO_2 and ACF/WO_3/TiO_2 composites for the degradation of the MO solution. The k_{app} value of the ACF/WO_3/TiO_2 sample is the largest, which is in accord with the photocatalytic activity.

WO_3/TiO_2 has a better degradation effect than pure TiO_2 because WO_3 is an energy sensitizer that improves the quantum efficiency and increases charge transfer. The TiO_2 deposited on the WO_3 surface can retain its photodegradation activity. When WO_3 (Eg = 2.8 eV) and TiO_2 (Eg = 3.2 eV) form a coupled photocatalyst, WO_3 can be excited by photons under visible illumination, and TiO_2 remains unexcited. Hole and electron pairs were generated and separated on the interface of WO_3 by visible light irradiation. The level of the conduction band in TiO_2 was lower than the reduction potential of WO_3. Therefore, the photogenerated electron with an interaction between WO_3 and TiO_2. The synergistic effect WO_3 and TiO_2 both promoted the separation efficiency of the photogenerated electron–hole pairs, resulting in the high photocatalytic activity of WO_3-hybridized TiO_2 samples. In this case, the WO_3 coupled TiO_2 system improved the reaction state.[39-43] Therefore, the WO_3 coupled TiO_2 had photocatalytic activity under visible light.

With a ACF/WO_3/TiO_2 system, the photocatalytic activites were enhanced mainly because of the high efficiency of the charge separation induced by the synergistic effect of ACF, WO_3 and TiO_2. Because WO_3 had the least band gap (0.5-3.2 eV), hole and electron pairs were generated and separated on the interface of WO_3 easily by visible light irradiation. Because both the conduction band (CB) and the valence band (VB) of WO_3 were higher than the CB and VB of TiO_2, when the hole

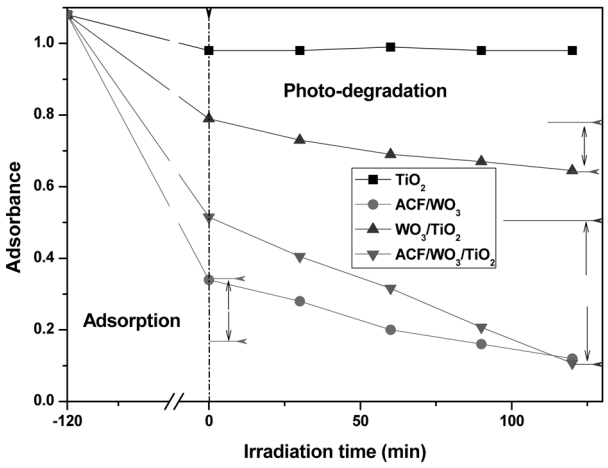

Fig. 4. Decolorization effect on MO of pure TiO_2, ACF/WO_3, WO_3/TiO_2 and ACF/WO_3/TiO_2.

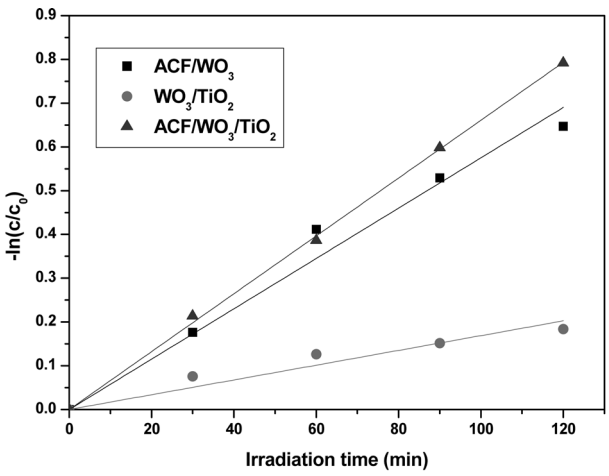

Fig. 5. Corresponding -ln (C/C_0) vs. t plots.

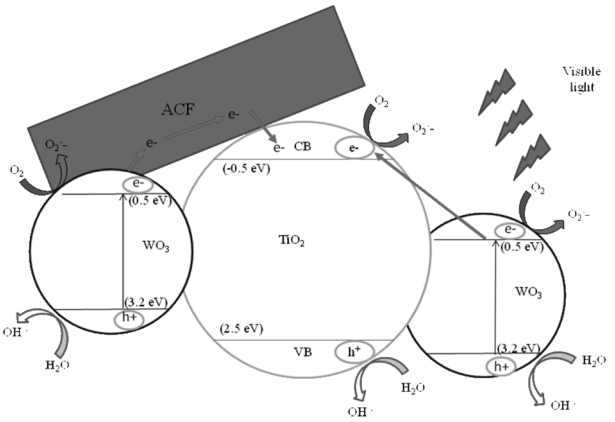

Fig. 6. Schematic diagram of the separation of photogenerated electrons and holes on the WO_3/TiO_2 interface.

and electron pairs also generated and separated on the interface of WO_3, the electrons at the CB of WO_3 migrated to the CB of TiO_2, and the holes at the VB of WO_3 migrated to the VB of TiO_2. This allowed the transfer of photogenerated electrons, which facilitated effective charge separation and decreased the rate of recombination about the electron-hole pairs. ACF acts as an adsorb effect and increases the surface area of the compounds, which can increase the adsorption effect for the samples, adsorb more O_2 and dye molecules, and make sure this systems takes full advantage of yield oxidizing species.[44-46]

Fig. 6 is the schematic diagram of the separation of photogenerated electrons and holes on the WO_3/TiO_2 interface.

The positive holes in the valence band can be trapped by OH or H_2O species adsorbed on the surface of the catalyst, producing reactive hydroxyl radicals in aqueous media. The photo-generated electrons accumulate on the surface of WO_3 and can be rapidly transferred to molecular oxygen O_2 to form the superoxide radical anion O_2^- and hydrogen peroxide H_2O_2. Oxidative degradation of azo dyes occurs by the attack of hydroxyl radicals and superoxide ions, which are highly reactive electrophilic oxidants. Due to the efficiency of hydroxyl radicals and superoxide ions, azo dyes were decompounded to CO_2, H_2O and inorganic compounds.[47-49]

4. Conclusions

This study examined the preparation and characterization of ACF/WO_3, WO_3/TiO_2 and ACF/WO_3/TiO_2. The BET surface area of ACF/WO_3 was higher than that of the ACF/WO_3/TiO_2 composite. XRD revealed a WO_3 structure and anatase. ACF/WO_3 exhibited a good photo-degradation effect under visible light irradiation, due to the photosensitive and enhancing BET surface area effect of ACF. The ACF/WO_3/TiO_2 composite showed the best photocatalytic degradation activity of the MO solution under visible light irradiation. This was attributed to three different effects, the photocatalytic reaction of the supported TiO_2, the energy transfer effects of ACF and WO_3, such as electrons and light, and the separation effect in this system.

REFERENCES

1. N. N. Lichtin, M. Avudathai, E. Berman, and A. Grayfer, "TiO_2-Photocatalyzed Oxidative Degradation of Binary Mixtures of Vaporized Organic Compounds," *Sol. Energy,* **56** 377-85 (1996).
2. C. Minero, E. Pelizzetti, S. Malato, and J. Blanco, "Large Solar Plant Photocatalytic Water Decontamination: Degradation of Atrazine," *Sol. Energy,* **56** 411-19 (1996).
3. L. A. Dibble and G. B. Raupp, "Fluidized-bed Photocatalytic Oxidation of Trichloroethylene in Contaminated Air Streams," *Environ. Sci. Technol.,* **28** 492-95 (1992).
4. A. Fujishima and K. Honda, "Electrochemical Photolysis of Water at a Semiconductor Electrode," *Nature,* **238** 37-8 (1972).
5. P. Ameta, R. Ameta, R. C. Ameta, and S. C. Ameta, "Use of Semiconductor Oxides in the Photocatalytic Reaction of Sodium Hexanitrocobaltate (III)," *J. Photochem. Photobilogy A: Chem.,* **103** 133-36 (1997).
6. Y. X. Li and F. Wasgestian, "Photocatalytic Reductionof Nitrate Ions on TiO_2 by Oxalic Acid," *J. Photochem. Photobiol. A: Chem.,* **112** 255-59 (1998).
7. K. T. Ranjit, R. Krishnamoorthy, and B. Viswanathan, "Photocatalytic Reduction of Nitrite and Nitrate on ZnS," *J. Photochem. Photobiol. A: Chem.,* **81** 55-8 (1994).
8. T. Huang, X. P. Lin, J. C. Xing, W. D. Wang, Z. C. Shan, and F. Q. Huang, "Photocatalytic Activities of Hetero-junction Semiconductors $WO_3/SrNb_2O_6$," *Mater. Sci. Eng. B,* **141** 49-54 (2007).
9. J. F. Porter and Y. G. Li, "Effect of Calcinations on the Microstructural Characteristic and Photoreactivity of Degussa P-25 TiO_2," *J. Mater. Sci.,* **34** 1523-31 (1999).
10. Y. Bessekhouad, N. Chaoui, M. Trzpit, N. Ghazzal, D. Robert, and J. V. Weber, "UV-vis Versus Visible Degradation of Acid Orange II in a Coupled CdS/TiO_2 Semiconductors Suspension," *J. Photochem. Photobiol. A,* **183** 218-24 (2006).
11. W. Xie, Y. Z. Li, W. Sun, J. C. Huang H. Xie, and X. J. Zhao, "Surface Modification of ZnO with Ag Imoroves Its Photocatalytic Efficiency and Photostability," *J. Photochem. Photobiol. A: Chem.,* **216** 2-3 (2010).
12. A. Fujishima, T. N. Rao, and D. A. Tryk, "Titanium Dioxide Photocatalysis," *J. Photochem. Photobiol. C,* 11-21 (2000).
13. M. R. Hoffmann, S. T. Martin, W. Y. Choi, and D. W. Bahnemann, "Environmental Applications of Semiconductor Photocatalysis," *Chem. Rev.,* **95** 69-96 (1995).
14. M. Asilturk, F. Saylkan, and E. Arpac, "Effect of Fe^{3+} Ion Doping to TiO_2 on the Photocatalytic Degradation of Malachite Green Dye Under UV and Vis-irradiation," *J. Photochem. Photobiol. A,* **203** 64-71 (2009).
15. M. Andersson, L. Osterlund, S. Ljungstrom, and A. Palmqvist, "Preparation of Nanosize Anatase and Rutile TiO_2 by Hydrothermal Treatment of Microemulsions and Their Activity for Photocatalytic Wet Oxidation of Phenol," *J. Phys. Chem. B,* **106** 10674-79 (2002).
16. H. Tada, A. Hattori, Y. Tokihisa, K. Imai, N. Tohge, and S. Ito, "A Patterned-TiO_2/SnO_2 Bilayer Type Photocatalyst," *J. Phys. Chem. B,* **104** 4585-87 (2000).
17. J. G. Yu, W. Liu, and H. G. Yu, "A One-pot Approach to Hierarchically Nanoporous Titania Hollow Microspheres with High Photocatalytic Activity," *Cryst. Growth Des.,* **8** 930-34 (2008).
18. T. Mori, J. Suzudi, K. Fujimoto, M. Watanabe, and Y. Hasegawa, "Reductive Decomposition of Nitrate Ion to Nitrogen in

Water on a Unque Hollandite Photocatalyst," *Appl. Catal. B,* **23** 283-89 (1999).
19. T. M. Wang, H. Y. Wang, P. Xu, X. C. Zhao, Y. L. Liu, and S. Chao, "The Effect of Properties of Semiconductor Oxide Thin Film on Photocatalytic Decomposition of Dyeing Waste Water," *Thin Solid Film,* **334** 103-8 (1998).
20. H. Kominami, A. Furusho, S. Murakami, H. Inoue, Y. Kera, and B. Ohtani, "Effective Photocatalytic Reduction of Nitrate to Ammonia in an Aqueous Suspension of Metal-loaded Titanium (IV) Oxide Particles in the Presence of Oxalic Acid," *Catal. Lett.,* **76** 31-4 (2001).
21. V. Iliev, D. Tomova, S. Rakovsky, A. Eliyas, and G. L. Puma, "Enhancement of Photocatalytic Oxidation of Oxalic Acid by Gold ModifiedWO_3/TiO_2 Photocatalysts Under UV and Visible Light Irradiation," *J. Mol. Catal. A: Chem.,* **327** 51-7 (2010).
22. V. Puddu, R. Mokaya, and G. L. Puma, "Novel One Step Hydrothermal Synthesis of TiO_2/WO_3 Nanocomposites with Enhanced Photocatalytic Activity," *Chem. Commun.,* **2007** 4749-51 (2007).
23. V. Keller, P. Bernhardt, and F. Garin, "Photocatalytic Oxidation of Butyl Acetate in Vapor Phase on TiO_2, Pt/TiO_2 and WO_3/TiO_2 Catalysts," *J. Catal.,* **215** 129-38 (2003).
24. X. Z. Li, F. B. Li, C. L. Yang, and W. K. Ge, "Photocatalytic Activity of WOx-TiO_2 under Visible Light Irradiation," *J. Photochem. Photobiol. A,* **141** 209-17 (2001).
25. H. Q. Wang, Z. B. Wu, and Y. Liu, "A Simple Two-step Template Approach for Preparing Carbon-doped Mesoporous TiO_2 Hollow Microspheres," *J. Phys. Chem. C,* **113** 13317-24 (2009).
26. E. J. Wolfrum, J. Huang, D. M. Blake, P. C. Maness, Z. Huang, J. Fiest, and W. A. Jacoby, "Photocatalytic Oxidation of Bacteria, Bacterial and Fungal Spores, and Model Biofilm Components to Carbon Dioxide on Titanium Dioxide-coated Surfaces," *Environ. Sci. Technol.,* **36** 3412-19 (2002).
27. S. U. M. Khan, M. Al-Shahry, and W.B. Ingler, "Efficient Photochemical Water Splitting by a Chemically Modified n-TiO_2," *Science,* **297** 2243-45 (2002).
28. X. W. Zhang, M. H. Zhou, and L. C. Lei, "Preparation of Photocatalytic TiO_2 Coating of Nanosized Particles Supported on Activated Carbon by AP-MOCVD," *Carbon,* **43** 1700-8 (2005).
29. C. C. Chan, C. C. Chang, W. C. Hsu, S. K. Wang, and J. Lin, "Photocatalytic Activities of Pd-loaded Mesoporous TiO_2 Thin Films," *Chem. Eng. J.,* **152** 492-7 (2009).
30. H. Gerischer and M. Lubke, "A Particle Size Effect in the Sensitization of TiO_2 Electrodes by a CdS Deposit," *J. Electroanal. Chem.,* **204** 225-7 (1986).
31. T. Sauer, G. Cesconeto Neto, H. J. Jose, and R. F. P. M. Moreira, "Kinetics of Photocatalytic Degradation of Reactive Dyes in a TiO_2 Slurry Reactor," *J. Photochem. Photobiol. A: Chem.,* **149** 147-54 (2002).
32. W. C. Oh, J. H. Son, F. J. Zhang, and M. L. Cheng, "Fabrication of Ni-AC/TiO_2 Composites and their Photocatalytic Activity for Degradation of Methylene Blue," *J. Kor. Ceram. Soc.,* **46** [1] 1-9 (2009).
33. Z. D. Meng, K. Zhang, and W. C. Oh, "Preparation of Different Fe Containing TiO_2 Photocatalysts and Comparision of Their Photocatalytic Activity," *Kor. J. Mater. Re.,* **20** 228-34 (2010).
34. D. N. Ke, H. J. Liu, T. Y. Peng, X. Liu, and K. Dai, "Preparation and Photocatalytic Activity of WO_3/TiO_2 Nanocomposite Particles," *Mater. Lett.,* **62** 447-50 (2008).
35. M. W. Xiao, L. S. Wang, X. J. Huang, Y. D. Wu, and Z. Dang, Synthesis and Characterization of WO_3/titanate Nanotubes Nanocomposite with Enhanced Photocatalytic Properties," *J. Alloys Compd.,* **470** 486-91 (2009).
36. K. K. Akurati, A. Vital, J. P. Dellemann, K. Michalow, T. Graule, D. Ferri, and A. Baiker, "Flame-madeWO_3/TiO_2 Nanoparticles: Relation Between Surface Acidity, Structure and Photocatalytic Activity," *Appl. Catal. B.,* **79** 53-62 (2008).
37. Saepurahman, M. A. Abdullah, and F. K. Chong, "Preparation and Characterization of Tungsten-loaded Titanium Dioxide Photocatalyst for Enhanced Dye Degradation," *J. Hazard. Mater.,* **176** 451-558 (2010).
38. J. Kasanen, M. Suvanto, and T. T. Pakkanen, "UV Stability of Polyurethane Binding Agent on Multilayer Photocatalytic TiO_2 Coating," *Polymer Testing,* **30** 381-9 (2011).
39. H. Yang, R. Shi, K. Zhang, Y. Hu, A. Tang, and X. Li, "Syn-Thesis of WO_3/TiO_2 Nanocomposites Via Sol-gel Method," *J. Alloys Compd.,* **398** 200-202 (2005).
40. A. Rampaul, I. P. Parkin, S. A. O' Neill, J. Desouza, A. Mills, and N. Elliot, "Titania and Tungsten Doped Titania Thin Films on Glass; Active Photocatalysts," *Polyhedron,* **22** 35-44 (2003).
41. M. R. Bayati, F. G. Fard, and A. Z. Moshfegh, "Visible Photodecomposition of Methylene Blue Over Micro Arc Oxidized WO_3 Loaded TiO_2 Nanaporous Layers," *Appl. Catal. A: Gen.,* **382** 322-31 (2010).
42. J. He, Q. Z. Cai, Y. G. Ji, H. H. Luo, D. J. Li, and B. Yu, "Influence of Fluorine on the Structure and Photocatalytic Activity of TiO_2 Film Prepared in Tungstate-electrolyte Via Micro-arc Oxidation," *J. Alloys Compd.,* **482** 476-81 (2009).
43. K. K. Akurati, A. Vital, J. P. Dellemann, K. M. Michalow, D. Ferri, T. Graule, and A. Baiker, "Flame-madeWO_3/TiO_2 Nanoparticles: Relation Between Surface Acidity, Structure and Photocatalytic Activity," *Appl. Catal. B: Environ.,* **79** 53-62 (2008).
44. J. C. Parker and R. W. Siegel, "Calibration of the Raman Spectrum to the Oxygen Stoichiometry of Nanophase, TiO_2," *Appl. Phys. Lett.,* **57** 943-5 (1990).
45. M. Fernandez-Garca, A. Martnez-Arias, A. Fuerte, and J. C. Conesa, "Nanostructured Ti-W Mixed-metal Oxides: Structural and Electronic Properties," *J. Phys. Chem. B,* **109** 6075-83 (2005).
46. C. Alcober, F. Alvarez, S. A. Bilmes, and R. J. Candal, "Photochromic W-TiO_2 Membranes, *J. Mater. Sci. Lett.,* **21** 501-504 (2002).
47. R. Asahi, T. Morikawa, T. Ohwaki, K. Aoki, and Y. Taga, "Visible-light Photocatalysis in Nitrogen-doped Titanium Oxides," *Science,* **293** 269-71 (2001).
48. V. Pore, M. Ritala, M. Leskela, S. Areva, M. Jarn, and J. Jarnstrom, "H_2S Modified Atomic Layer Deposition Process for Photocatalytic TiO_2 Thin Films," *J. Mater. Chem.,* **17** 1361-71 (2007).
49. Z. D. Meng, L. Zhu, J. G. Choi, M. L. Chen, and W. C. Oh, "Effect of Pt Treated Fullerene/TiO_2 on the Photocatalytic Degradation of MO Under Visible Light," *J. Mater. Chem.,* **21** 7596-603 (2011).